PHYSICAL REVIEW B **96**, 060403(R) (2017)

Finite-temperature dynamics and thermal intraband magnon scattering in Haldane spin-one chains

J. Becker,[1] T. Köhler,[2] A. C. Tiegel,[2] S. R. Manmana,[2] S. Wessel,[1] and A. Honecker[3]
[1]*Institut für Theoretische Festkörperphysik, JARA-FIT and JARA-HPC, RWTH Aachen University, 52056 Aachen, Germany*
[2]*Institut für Theoretische Physik, Georg-August-Universität Göttingen, 37077 Göttingen, Germany*
[3]*Laboratoire de Physique Théorique et Modélisation, CNRS UMR 8089, Université de Cergy-Pontoise, 95302 Cergy-Pontoise Cedex, France*
(Received 23 March 2017; revised manuscript received 29 May 2017; published 3 August 2017)

The antiferromagnetic spin-one chain is considerably one of the most fundamental quantum many-body systems, with symmetry-protected topological order in the ground state. Here, we present results for its dynamical spin structure factor at finite temperatures, based on a combination of exact numerical diagonalization, matrix-product-state calculations, and quantum Monte Carlo simulations. Open finite chains exhibit a subgap band in the thermal spectral functions, indicative of localized edge states. Moreover, we observe the thermal activation of a distinct low-energy continuum contribution to the spin spectral function with an enhanced spectral weight at low momenta and its upper threshold. This emerging thermal spectral feature of the Haldane spin-one chain is shown to result from intraband magnon scattering due to the thermal population of the single-magnon branch, which features a large bandwidth-to-gap ratio. These findings are discussed with respect to possible future studies on spin-one chain compounds based on inelastic neutron scattering.

DOI: 10.1103/PhysRevB.96.060403

One-dimensional quantum spin models constitute basic condensed matter many-body systems that despite their simplicity exhibit a rich variety of emergent phenomena [1]. These include the formation of collective excitations and nonclassical ground states with characteristic patterns in the quantum entanglement. From this perspective, Haldane's conjecture [2–4] on a fundamental difference in the low-energy physics of integer-valued spin chains with respect to the spin-half Heisenberg chain has established the spin-one chain model as a fundamental spin system, which furthermore finds realizations in various, mainly Ni^{2+}-based compounds [5–17]. Its properties have been intensively explored in both theoretical and numerical, as well as experimental studies in recent years, mainly with a focus toward the peculiar properties of the gapped ground state [18,19], which is now understood as a most basic instance of symmetry-protected topological (SPT) order [20,21]. This leads, e.g., to the formation of a pair of entangled spin-half low-energy edge states for open finite chains [22].

Dynamical probes of quantum magnetism in spin-one chain compounds, performed using inelastic neutron scattering, have confirmed the gapped magnetic excitation spectrum [6,15,23–27]. At low temperatures, the corresponding dynamical spin structure factor is dominated by the gapped single-magnon branch, with additional contributions from multimagnon continuum states, leading to the termination of the single-magnon branch due to decay and scattering with the two-magnon continuum states [28–46] (cf. Fig. 1 for an illustration). The effects of thermal fluctuations on the dynamical spin structure factor at elevated temperatures [15,47,48] have been less intensively investigated theoretically, in particular in the region of intermediate energy scales, where theoretical approaches require one to account for both quantum and thermal fluctuations. Previous theoretical works mainly focused on the temperature-induced shift in the single-magnon dispersion as well as its thermal broadening in the low-temperature regime [49–54].

In this Rapid Communication, we discuss the emergence of a distinct, thermal contribution to the finite-temperature dynamical spin structure factor that we find to result from intraband magnon scattering (IBMS) (cf. Fig. 1). The IBMS continuum exhibits an enhanced spectral weight near its upper edge, resulting from the van Hove singularity in the density of states near the extrema of the single-magnon band. This enhanced spectral weight appears close to the single-magnon branch due to the large bandwidth of the latter. Our results furthermore indicate that this thermal IBMS may feasibly be detected upon performing neutron scattering experiments in a temperature regime of the order of the spin gap. In addition, we find a signature of an edge-state mode for open chains, which is visible over an extended temperature region.

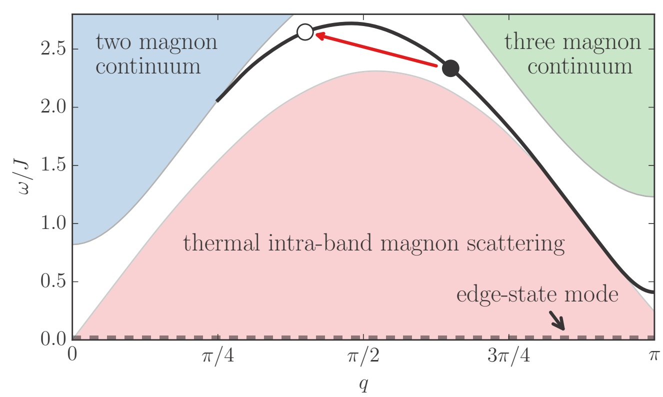

FIG. 1. Sketch of the low-energy excitations of the Haldane spin-one chain. The black line shows the gapped single-magnon dispersion, and the upper shaded regions denote the two- and three-magnon continua. The lower shaded region encloses the intraband-magnon-scattering contribution to the dynamical spin structure factor that emerges from the thermal population of the single-magnon branch. For open chains, an additional subgap edge-state mode extends from $q = \pi$ toward smaller momenta, indicated by the dashed line.

Before presenting our results for the dynamical spin structure factor, we first introduce the model and the employed numerical methods. The Hamiltonian for the SU(2)-symmetric antiferromagnetic spin-one chain of length L reads

$H = J\sum_{\langle i,j\rangle} \mathbf{S}_i \cdot \mathbf{S}_j$, with $J > 0$, where in the following we employ both open chains (OBC) and closed chains with periodic boundary conditions (PBC). The dynamical spin structure factor is given in the Heisenberg picture as $S(q,\omega) = \int dt\, e^{-i\omega t}\langle \mathbf{S}_q(t)\cdot \mathbf{S}_{-q}(0)\rangle$, where $\mathbf{S}_q = \frac{1}{\sqrt{L}}\sum_j e^{-iqj}\mathbf{S}_j$, with $q = 2\pi\nu/L$, $\nu = 1,2,\ldots,L$ for PBC. Using numerical exact diagonalization (ED), we were able to obtain numerically exact results for $S(q,\omega)$ on finite chains with PBC up to $L = 20$ [55–60]. In order to access larger system sizes, we used both density-matrix renormalization group (DMRG) [34,35,61] and quantum Monte Carlo (QMC) [62] approaches to calculate $S(q,\omega)$. For the DMRG-based analysis we used a recently developed finite-temperature approach [63], formulated within matrix product states (MPS) [64], which works directly in the frequency domain. As is the case for other finite-temperature time-dependent DMRG algorithms [65–67], this method is based on the purification of the thermal density operator obtained via imaginary time evolution. However, the underlying thermofield formalism [68] in combination with Liouville-space dynamics [69] allows us to naturally work in the frequency domain and thus apply a moment expansion in terms of Chebyshev polynomials to the spectral function itself [70–72]. Working with OBC in the DMRG calculations for efficiency reasons, the momentum-space spin operators are related to those in real space via $\mathbf{S}_q = \sqrt{\frac{2}{L+1}}\sum_{j=1}^{L}\sin(qj)\mathbf{S}_j$, where $q = \pi\nu/(L+1)$, $\nu = 1,2,\ldots,L$ [73]. We typically consider a chain length of $L = 32$ and an MPS truncation at bond dimension $m = 250$ which yields compression errors $\mathcal{O}(10^{-2})$. The iterative Chebyshev expansion is truncated at order 2000, which results in an estimated broadening σ_ω, weakly frequency dependent, of the order of $0.1J$. For the QMC calculations we used the stochastic series expansion (SSE) algorithm with a generalized directed loop update [74,75], and both OBC and PBC can be considered equally well. In order to access the spin dynamics, correlation functions in Matsubara frequency space, $C(q,i\omega_n) = \int_0^\beta d\tau\, e^{i\omega_n\tau}\langle \mathbf{S}_q(\tau)\cdot\mathbf{S}_{-q}(0)\rangle$, with $\omega_n = 2\pi n/\beta$, $n \in \mathbb{N}_0$ are measured, utilizing a mapping of the SSE configuration space to continuous imaginary time [76,77]. Here, $\beta = 1/T$, and we typically require up to the 200 lowest Matsubara frequencies. Real-frequency spectra are then obtained by performing an analytic continuation to invert the relation $C(q,i\omega_n) = \int_0^\infty d\omega\, \frac{\omega}{\pi}\frac{1-e^{-\beta\omega}}{\omega_n^2+\omega^2}S(q,\omega)$. To this end, we employ a stochastic analytic continuation algorithm [78] which yields Monte Carlo averages over ensembles of proposed spectral functions.

An overview of our main findings, the spectral function $S(q,\omega)$ of the spin-one chain at different temperatures, is provided in Fig. 2, where the left (right) column shows DMRG (QMC) results for a chain with OBC (PBC). A comparison of the DMRG spectral functions at a set of fixed momenta and for different temperatures is also available [56]. The data obtained by our finite-temperature schemes at $T/J = 1/24$ [panels (a) and (b)] effectively represents ground-state results. The most prominent contribution to $S(q,\omega)$ is the single-magnon branch, with a lowest excitation gap of $\Delta \approx 0.41J$ at the antiferromagnetic wave vector, $q = \pi$ [28,36,38]. Near $q = \pi/4$, the magnon branch merges into the two-magnon continuum, leading to the decay of elementary magnon excitations [36,44,45]. Correspondingly, in the low-q region,

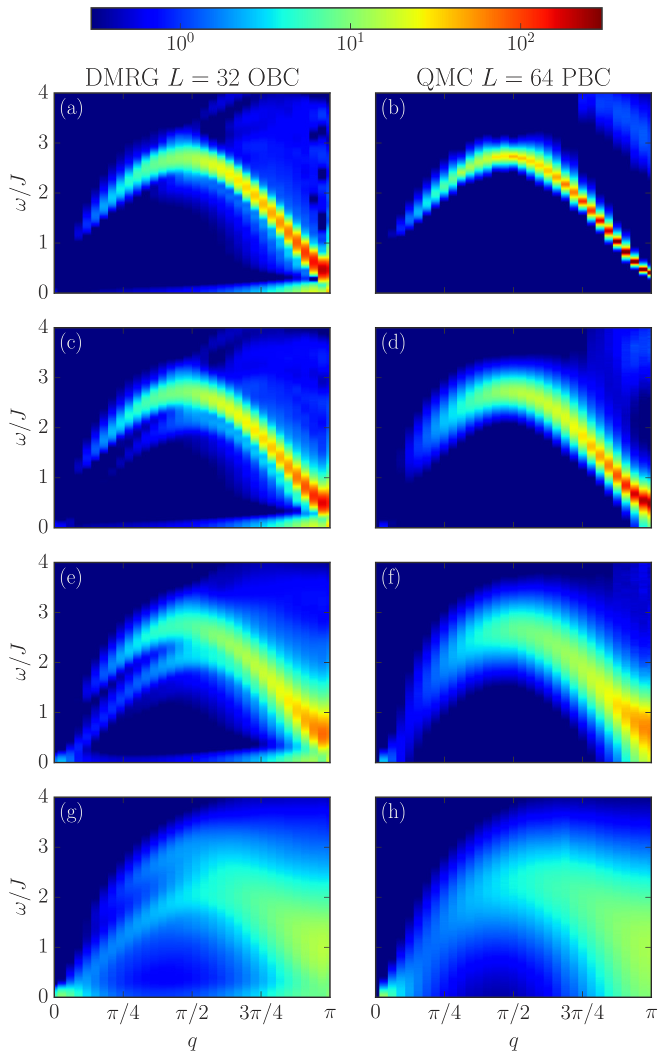

FIG. 2. Dynamical spin structure factor $S(q,\omega)$ for the Haldane spin-one chain from DMRG with OBC (left panels), and QMC with PBC (right panels) for various temperatures T (a,b) $T/J = 1/24$, (c,d) $T/J = 0.2$, (e,f) $T/J = 0.4$, and (g,h) $T/J = 1.0$.

we observe a loss of spectral weight. For a finite system with OBC [cf. Fig. 2(a)], a distinct additional contribution to the spin dynamics results from the low-energy edge states located at the two ends of an open spin-one chain [22]. Due to the local character of the edge-state contribution, this low-energy spectral weight vanishes proportional to $1/L$ upon increasing the system size. This is confirmed by a finite-size analysis of the total spectral weight in the subgap region [56]. In calculations with PBC, this subgap feature is absent [cf. Fig. 2(b)], while for chains with OBC we also obtain it from QMC [56]. The DMRG spectral function in Fig. 2(a) shows a tiny fraction of the spectral weight which is spread both below and above the single-magnon branch. This results mainly from the truncation of the Chebyshev expansion and the comparatively small MPS bond dimension, and is not observed in the QMC simulations. The QMC spectrum in Fig. 2(b) thus allows us to also resolve the well-separated three-magnon continuum near $q = \pi$, where its intensity is sufficiently large [56].

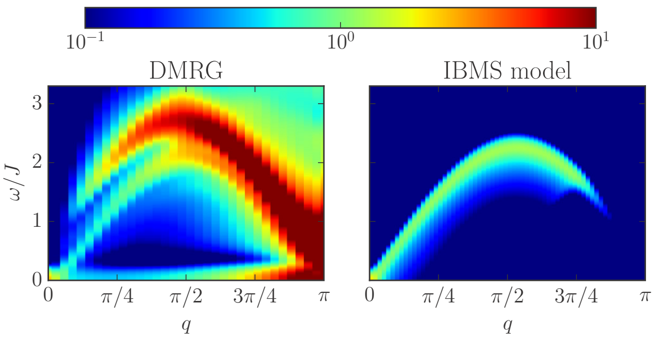

FIG. 3. Comparison of the DMRG spectral function $S(q,\omega)$ (left panel) for $L = 32$ (OBC) with $S^{IB}(q,\omega)$ calculated for the IBMS model (right panel) at $T/J = 0.3$. A Gaussian broadening with $\sigma_\omega = 0.1J$, similar to the DMRG spectra, was applied to the IBMS model spectral function.

We next consider the thermal effects on the dynamical spin structure factor [cf. Figs. 2(c)–2(h)], as well as Fig. 3. The thermal broadening of the single-magnon branch as well as the thermal band narrowing has been examined previously [49,50,52] (cf. also Ref. [56]). The OBC spectra furthermore show that the open finite-system's edge-state contribution to the dynamical spin structure factor remains a distinct subgap feature also at finite temperatures, which thus provides a convenient fingerprint of the SPT nature of the ground state.

A qualitative change seen only in the finite-T spectral function is the emergence of additional spectral weight below the single-magnon branch for $T \gtrsim \Delta/2 \approx 0.2J$, which is well separated from the single-magnon branch for $q \lesssim \pi/2$. At $T = 0.4J$ [cf. Fig. 2(e)], this temperature-induced spectral weight still appears to resemble a dispersing mode, softening at $q = 0$, where the spectral weight is further enhanced. While the DMRG approach allows us to distinguish this temperature-induced spectral weight from the single-magnon branch, the spectral function obtained from the analytically continued QMC data [cf. Fig. 2(f)] is affected by a difficulty of the analytic continuation to separate such closely spaced spectral weight contributions at finite temperatures. The QMC data nevertheless exhibit the presence of the thermal spectral weight contribution at low energies, close to $q = 0$. Upon further increasing the temperature, a redistribution of the spectral weight can be seen in Fig. 2, and this eventually reveals the actual character of the temperature-induced spectral feature, which forms an extended continuum with an enhanced spectral weight at its upper threshold [cf. Figs. 2(g) and 2(h)].

This thermal spectral weight results from IBMS processes that have been previously observed in dimerized spin-1/2 chains [79–81]: the thermal population of the magnon mode, predominantly in the vicinity of $q = \pi$, where the magnon dispersion has its lowest excitation gap, allows for scattering processes of a thermally excited magnon to another state on the single-magnon branch (cf. the illustration in Fig. 1). Such processes contribute to $S(q,\omega)$ upon respecting the conservation of momentum and energy exchange with the scattering particle (such as, e.g., in neutron scattering). More quantitatively, this thermal IBMS contribution $S^{IB}(q,\omega)$ to the dynamical spin structure factor can be approximately obtained using a magnon-state representation within a basic kinematic model. We denote by $|k,\sigma\rangle$ a single-magnon ($S_{\text{tot}} = 1$) excitation of momentum k and $S^z_{\text{tot}} = \sigma \in \{0, \pm 1\}$ atop the $S_{\text{tot}} = 0$ ground state $|0\rangle$, with an excitation energy ϵ_k along the single-magnon branch. The multimagnon states are subject to a hard-core constraint that can be treated in several approximate ways that all yield the same low-temperature asymptotics. We found it convenient to use a k-space-based hard-core boson approximation of the initial (i) and final (f) states in the Lehmann representation of $S(q,\omega) = 3\sum_{i,f} e^{-\beta E_i}/Z\,|\langle f|S^z_q|i\rangle|^2\delta(\omega - E_f + E_i)$. Here, the factor of 3 accounts for the SU(2) symmetry of the Hamiltonian H. Neglecting further interaction effects, E_i (E_f) equals the sum of the occupied single-magnon state energies in the initial (final) state, and the partition function $Z = \prod_{k,\sigma}(1 + e^{-\beta\epsilon_k})$. The leading-order scattering processes, whereby a thermally excited magnon is scattered into another unoccupied single-magnon state, then yield

$$S^{IB}(q,\omega) = 3\sum_{k,\sigma}\frac{|\langle k+q,\sigma|S^z_q|k,\sigma\rangle|^2}{(1+e^{\beta\epsilon_k})(1+e^{-\beta\epsilon_{k+q}})}\delta(\omega - \epsilon_{k+q} + \epsilon_k).$$

Finally, we approximate the nonvanishing scattering matrix elements as $|\langle k+q,\pm 1|S^z_q|k,\pm 1\rangle|^2 \approx 1/L$, which would hold exactly, if the single-magnon states were obtained as $|k,\pm 1\rangle = S^\pm_k|0\rangle$ and $S^z_q|k,0\rangle = 0$, using that $[S^z_q, S^\pm_k] = \pm S^\pm_{k+q}$, with $S^\pm_q = \frac{1}{\sqrt{L}}\sum_j e^{-iqj}S^\pm_j$. The overall $1/L$ scaling of the matrix elements renders $S^{IB}(q,\omega)$ convergent in the thermodynamic limit. In addition to the above explicit treatment of the longitudinal (S^z_q) channel, one can also perform a similar calculation for the transverse sectors of $S^{IB}(q,\omega)$, which then indeed exhibits its anticipated SU(2) symmetry.

We evaluated the IBMS contribution from this basic model, based on the single-magnon dispersion taken from Ref. [45]. The resulting IBMS spectral function at $T/J = 0.3$ is shown in the right panel of Fig. 3, next to the corresponding DMRG result for $S(q,\omega)$. Here, we convoluted the IBMS model spectral function with a Gaussian resolution of width $\sigma_\omega = 0.1J$, i.e., the broadening in the DMRG spectral functions. We find that our rather simple model qualitatively captures the shape of the IBMS contribution, in particular its upper boundary. Near this threshold, as well as near $q = 0$, the spectral weight is enhanced due to the van Hove singularity in the magnon density of states near $k = \pi/2$ and π. The full extent of the IBMS continuum as obtained within the IBMS model is indicated in Fig. 1. Within the maximum energy regime $\omega/J \approx 2$ of the IBMS signal near $q = \pi/2$, where finite-size effects are expected to be weakest, we can use the $L = 20$ ED data for a more detailed comparison, since in the ED approach, we can choose a smaller broadening $\sigma_\omega = 0.05J$. A comparison of the ED spectral functions for $q = \pi/2$ and $q = 0.4\pi$ to the IBMS model is shown in Fig. 4 for $T/J = 0.3$.

For $q = \pi/2$, where we can directly compare ED data for $L = 20$ and $L = 16$ (since for both chain lengths, $q = \pi/2$ is an available lattice momentum) we conclude that indeed the $L = 20$ data in the relevant energy region exhibit only weak residual finite-size effects. By a direct comparison to the $T = 0$ data, we identify the thermally induced spectral

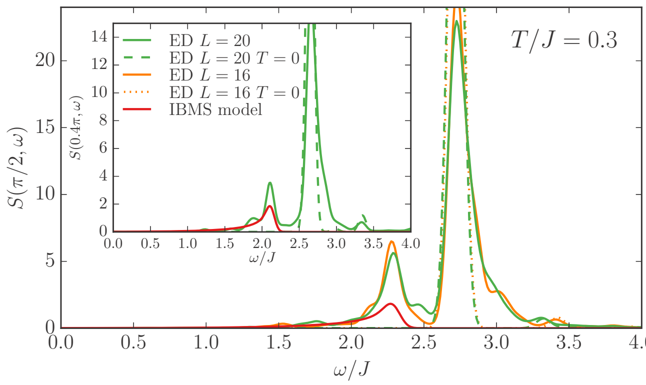

FIG. 4. Comparison of the ED spectral functions $S(q,\omega)$ with the IBMS model for $S^{IB}(q,\omega)$ at $T/J = 0.3$. The main panel shows results for $q = \pi/2$, and the inset those for $q = 0.4\pi$. For comparison, ED results for $T = 0$ are also included. A Gaussian broadening with $\sigma_\omega = 0.05J$ was applied to all spectral functions in this figure.

weight, with a peak at $\omega/J \approx 2.3$, and clearly separated from the magnon peak at $\omega/J \approx 2.7$. The position of the thermal peak is well reproduced by the IBMS model. To compare the corresponding spectral weight in the ED data to the IBMS model, one needs to account for the additional weight in the ED spectral function that is due to the broadened magnon peak; this elevates the IBMS signal in the ED data as compared to the background-free IBMS model. A similar comparison for $q = 0.4\pi$, a momentum that is accessible on the $L = 20$ chain, is shown in the inset of Fig. 4. Also here, we observe that the IBMS contribution to the ED spectral function is well reproduced by the IBMS model. While the above basic kinematic model already captures the overall properties of the IBMS contribution to $S(q,\omega)$, it would nevertheless be interesting to account for direct magnon-magnon interactions. As mentioned above, these lead to band narrowing and broadening of the single-magnon mode at finite temperatures and should be accounted for in a more thorough analytical description of the IBMS process. Furthermore, our approximate treatment of the scattering matrix elements renders the ω-integrated IBMS spectral weight less q dependent than observed in the numerical results, which show an overall increase in the IBMS signal for increasing finite values of q (cf. Figs. 2 and 3). Nevertheless, our basic model clearly demonstrates the mechanism behind the IBMS contribution to the dynamical spin structure factor at finite temperatures.

Thermally activated IBMS scattering is expected to be a general phenomenon in gapped quantum magnets, and indeed it is known from dimerized spin-1/2 chains [79–81]. The case of the Haldane spin-one chain that we have investigated in the present Rapid Communication is characterized by a large bandwidth as compared to the gap such that the maximum intensity of the IBMS continuum appears close to the single-magnon mode. In the present case, the IBMS thus provides an important contribution to the finite-temperature spin dynamics at low-to-intermediate scattering momenta. It would be interesting to identify the thermal IBMS signal from the scattering intensity in inelastic neutron scattering experiments on spin-one chain compounds. We anticipate the IBMS signal to be well accessible within a temperature regime set by the spin excitation gap. It may, however, be important to examine the influence of a single-ion anisotropy and interchain couplings on the IBMS signal. Furthermore, we expect the reduction of the spin gap by an applied magnetic field to enhance the IBMS signal toward lower temperatures, eventually making it relevant for the zero-temperature longitudinal response when the Haldane gap closes.

We thank S. Capponi, A. E. Feiguin, B. Lake, B. Normand, A. W. Sandvik, and O. F. Syljuåsen for useful discussions. This work was supported by the DFG research unit FOR1807, the CRC 1073 (Project B03), and the Helmholtz Virtual Institute “New states of matter and their excitations” (Project No. VH-VI-521). We acknowledge the allocation of CPU time at JSC Jülich and RWTH Aachen University via JARA-HPC.

[1] H.-J. Mikeska and A. K. Kolezhuk, One-dimensional magnetism, Lect. Notes Phys. **645**, 1 (2004).

[2] F. D. M. Haldane, Ground state properties of antiferromagnetic chains with unrestricted spin: Integer spin chains as realisations of the O(3) non-linear sigma model, ILL preprint SP-81/95, 1981 (unpublished), see also arXiv:1612.00076.

[3] F. D. M. Haldane, Nonlinear Field Theory of Large-Spin Heisenberg Antiferromagnets: Semiclassically Quantized Solitons of the One-Dimensional Easy-Axis Néel State, Phys. Rev. Lett. **50**, 1153 (1983).

[4] F. D. M. Haldane, Continuum dynamics of the 1-D Heisenberg antiferromagnet: Identification with the O(3) nonlinear sigma model, Phys. Lett. A **93**, 464 (1983).

[5] W. J. L. Buyers, R. M. Morra, R. L. Armstrong, M. J. Hogan, P. Gerlach, and K. Hirakawa, Experimental Evidence for the Haldane Gap in a Spin-1 Nearly Isotropic, Antiferromagnetic Chain, Phys. Rev. Lett. **56**, 371 (1986).

[6] M. Steiner, K. Kakurai, J. K. Kjems, D. Petitgrand, and R. Pynn, Inelastic neutron scattering studies on 1D near-Heisenberg antiferromagnets: A test of the Haldane conjecture, J. Appl. Phys. **61**, 3953 (1987).

[7] J. P. Renard, M. Verdaguer, L. P. Regnault, W. A. C. Erkelens, J. Rossat-Mignod, and W. G. Stirling, Presumption for a quantum energy gap in the quasi-one-dimensional $S = 1$ Heisenberg antiferromagnet $Ni(C_2H_8N_2)_2NO_2(ClO_4)$, Europhys. Lett. **3**, 945 (1987).

[8] J. P. Renard, M. Verdaguer, L. P. Regnault, W. A. C. Erkelens, J. Rossat-Mignod, J. Ribas, W. G. Stirling, and C. Vettier, Quantum energy gap in two quasi-one-dimensional $S = 1$ Heisenberg antiferromagnets (invited), J. Appl. Phys. **63**, 3538 (1988).

[9] L. P. Regnault, I. Zaliznyak, J. P. Renard, and C. Vettier, Inelastic-neutron-scattering study of the spin dynamics in the Haldane-gap system $Ni(C_2H_8N_2)_2NO_2ClO_4$, Phys. Rev. B **50**, 9174 (1994).

[10] M. Orendáč, A. Orendáčová, J. Černák, A. Feher, P. J. C. Signore, M. W. Meisel, S. Merah, and M. Verdaguer, Thermodynamic and magnetic properties of the $S = 1$ Heisenberg chain

$Ni(C_2H_8N_2)_2Ni(CN)_4$: Experiments and theory, Phys. Rev. B **52**, 3435 (1995).
[11] M. Takigawa, T. Asano, Y. Ajiro, M. Mekata, and Y. J. Uemura, Dynamics in the $S = 1$ One-Dimensional Antiferromagnet $AgVP_2S_6$ via ^{31}P and ^{51}V NMR, Phys. Rev. Lett. **76**, 2173 (1996).
[12] G. Xu, J. F. DiTusa, T. Ito, K. Oka, H. Takagi, C. Broholm, and G. Aeppli, Y_2BaNiO_5: A nearly ideal realization of the $S = 1$ Heisenberg chain with antiferromagnetic interactions, Phys. Rev. B **54**, R6827 (1996).
[13] Z. Honda, H. Asakawa, and K. Katsumata, Magnetic Field versus Temperature Phase Diagram of a Quasi-One-Dimensional $S = 1$ Heisenberg Antiferromagnet, Phys. Rev. Lett. **81**, 2566 (1998).
[14] A. Zheludev, Y. Chen, C. L. Broholm, Z. Honda, and K. Katsumata, Haldane-gap excitations in the low-H_c one-dimensional quantum antiferromagnet $Ni(C_5D_{14}N_2)_2N_3(PF_6)$, Phys. Rev. B **63**, 104410 (2001).
[15] G. Xu, C. Broholm, Y.-A. Soh, G. Aeppli, J. F. DiTusa, Y. Chen, M. Kenzelmann, C. D. Frost, T. Ito, K. Oka, and H. Takagi, Mesoscopic phase coherence in a quantum spin fluid, Science **317**, 1049 (2007).
[16] A. Niazi, S. L. Bud'ko, D. L. Schlagel, J. Q. Yan, T. A. Lograsso, A. Kreyssig, S. Das, S. Nandi, A. I. Goldman, A. Honecker, R. W. McCallum, M. Reehuis, O. Pieper, B. Lake, and D. C. Johnston, Single-crystal growth, crystallography, magnetic susceptibility, heat capacity, and thermal expansion of the antiferromagnetic $S = 1$ chain compound CaV_2O_4, Phys. Rev. B **79**, 104432 (2009).
[17] O. Pieper, B. Lake, A. Daoud-Aladine, M. Reehuis, K. Prokeš, B. Klemke, K. Kiefer, J. Q. Yan, A. Niazi, D. C. Johnston, and A. Honecker, Magnetic structure and interactions in the quasi-one-dimensional antiferromagnet CaV_2O_4, Phys. Rev. B **79**, 180409(R) (2009).
[18] M. den Nijs and K. Rommelse, Preroughening transitions in crystal surfaces and valence-bond phases in quantum spin chains, Phys. Rev. B **40**, 4709 (1989).
[19] T. Kennedy and H. Tasaki, Hidden symmetry breaking and the Haldane phase in $S = 1$ quantum spin chains, Commun. Math. Phys. **147**, 431 (1992).
[20] Z.-C. Gu and X.-G. Wen, Tensor-entanglement-filtering renormalization approach and symmetry-protected topological order, Phys. Rev. B **80**, 155131 (2009).
[21] F. Pollmann, A. M. Turner, E. Berg, and M. Oshikawa, Entanglement spectrum of a topological phase in one dimension, Phys. Rev. B **81**, 064439 (2010).
[22] T. Kennedy, Exact diagonalisations of open spin-1 chains, J. Phys.: Condens. Matter **2**, 5737 (1990).
[23] S. Ma, C. Broholm, D. H. Reich, B. J. Sternlieb, and R. W. Erwin, Dominance of Long-Lived Excitations in the Antiferromagnetic Spin-1 Chain NENP, Phys. Rev. Lett. **69**, 3571 (1992).
[24] R. A. Cowley, M. Kenzelmann, W. J. L. Buyers, D. F. McMorrow, R. Coldea, and M. Enderle, New results on the excitations of an $S = 1$ quantum chain, J. Magn. Magn. Mater. **226-230**, 437 (2001).
[25] I. A. Zaliznyak, S.-H. Lee, and S. V. Petrov, Continuum in the Spin-Excitation Spectrum of a Haldane Chain Observed by Neutron Scattering in $CsNiCl_3$, Phys. Rev. Lett. **87**, 017202 (2001).
[26] M. Kenzelmann, R. A. Cowley, W. J. L. Buyers, Z. Tun, R. Coldea, and M. Enderle, Properties of Haldane excitations and multiparticle states in the antiferromagnetic spin-1 chain compound $CsNiCl_3$, Phys. Rev. B **66**, 024407 (2002).
[27] A. K. Bera, B. Lake, A. T. M. N. Islam, B. Klemke, E. Faulhaber, and J. M. Law, Field-induced magnetic ordering and single-ion anisotropy in the quasi-one-dimensional Haldane chain compound $SrNi_2V_2O_8$: A single-crystal investigation, Phys. Rev. B **87**, 224423 (2013).
[28] M. P. Nightingale and H. W. J. Blöte, Gap of the linear spin-1 Heisenberg antiferromagnet: A Monte Carlo calculation, Phys. Rev. B **33**, 659(R) (1986).
[29] M. Takahashi, Monte Carlo Calculation of Elementary Excitation of Spin Chains, Phys. Rev. Lett. **62**, 2313 (1989).
[30] G. Gómez-Santos, Variational Approach to the XXZ Spin-1 Linear Chain: Elementary Excitations and Haldane Conjecture, Phys. Rev. Lett. **63**, 790 (1989).
[31] T. Sakai and M. Takahashi, Energy gap of the $S = 1$ antiferromagnetic Heisenberg chain, Phys. Rev. B **42**, 1090(R) (1990).
[32] J. Deisz, M. Jarrell, and D. L. Cox, $S(q,\omega)$ for the $S = \frac{1}{2}$ and $S = 1$ one-dimensional Heisenberg antiferromagnet: A quantum Monte Carlo study, Phys. Rev. B **42**, 4869(R) (1990).
[33] I. Affleck and R. A. Weston, Theory of near-zero-wave-vector neutron scattering in Haldane-gap antiferromagnets, Phys. Rev. B **45**, 4667 (1992).
[34] S. R. White, Density Matrix Formulation for Quantum Renormalization Groups, Phys. Rev. Lett. **69**, 2863 (1992).
[35] S. R. White, Density-matrix algorithms for quantum renormalization groups, Phys. Rev. B **48**, 10345 (1993).
[36] S. R. White and D. A. Huse, Numerical renormalization-group study of low-lying eigenstates of the antiferromagnetic $S = 1$ Heisenberg chain, Phys. Rev. B **48**, 3844 (1993).
[37] S. V. Meshkov, Monte Carlo study of quantum spin chains, Phys. Rev. B **48**, 6167 (1993).
[38] O. Golinelli, Th. Jolicœur, and R. Lacaze, Finite-lattice extrapolations for a Haldane-gap antiferromagnet, Phys. Rev. B **50**, 3037 (1994).
[39] S. Yamamoto and S. Miyashita, Low-lying excitations in the $S = 1$ antiferromagnetic Heisenberg chain, Phys. Lett. A **235**, 545 (1997).
[40] A. Schmitt, K.-H. Mütter, M. Karbach, Y. Yu, and G. Müller, Static and dynamic structure factors in the Haldane phase of the bilinear-biquadratic spin-1 chain, Phys. Rev. B **58**, 5498 (1998).
[41] M. D. P. Horton and I. Affleck, Three-magnon contribution to the spin correlation function in integer-spin antiferromagnetic chains, Phys. Rev. B **60**, 11891 (1999).
[42] F. H. L. Essler, Three-particle scattering continuum in quasi-one-dimensional integer-spin Heisenberg magnets, Phys. Rev. B **62**, 3264 (2000).
[43] M. Kenzelmann, R. A. Cowley, W. J. L. Buyers, R. Coldea, J. S. Gardner, M. Enderle, D. F. McMorrow. and S. M. Bennington, Multiparticle States in the $S = 1$ Chain System $CsNiCl_3$, Phys. Rev. Lett. **87**, 017201 (2001).
[44] A. Kolezhuk and S. Sachdev, Magnon Decay in Gapped Quantum Spin Systems, Phys. Rev. Lett. **96**, 087203 (2006).
[45] S. R. White and I. Affleck, Spectral function for the $S = 1$ Heisenberg antiferromagetic chain, Phys. Rev. B **77**, 134437 (2008).

[46] Y. Rahnavard and W. Brenig, Spin dynamics of the anisotropic spin-1 antiferromagnetic chain at finite magnetic fields, Phys. Rev. B **91**, 054405 (2015).
[47] M. Kenzelmann, R. A. Cowley, W. J. L. Buyers, and D. F. McMorrow, Temperature evolution of the quantum gap in $CsNiCl_3$, Phys. Rev. B **63**, 134417 (2001).
[48] M. Kenzelmann and P. Santini, Temperature dependence of single particle excitations in a $S = 1$ chain: Exact diagonalization calculations compared to neutron scattering experiments, Phys. Rev. B **66**, 184429 (2002).
[49] Th. Jolicœur and O. Golinelli, σ-model study of Haldane-gap antiferromagnets, Phys. Rev. B **50**, 9265 (1994).
[50] K. Damle and S. Sachdev, Spin dynamics and transport in gapped one-dimensional Heisenberg antiferromagnets at nonzero temperatures, Phys. Rev. B **57**, 8307 (1998).
[51] M. Kenzelmann, R. A. Cowley, W. J. L. Buyers, R. Coldea, M. Enderle, and D. F. McMorrow, Evolution of spin excitations in a gapped antiferromagnet from the quantum to the high-temperature limit, Phys. Rev. B **66**, 174412 (2002).
[52] O. F. Syljuåsen, Using the average spectrum method to extract dynamics from quantum Monte Carlo simulations, Phys. Rev. B **78**, 174429 (2008).
[53] F. H. L. Essler and R. M. Konik, Finite-temperature lineshapes in gapped quantum spin chains, Phys. Rev. B **78**, 100403(R) (2008).
[54] F. H. L. Essler and R. M. Konik, Finite-temperature dynamical correlations in massive integrable quantum field theories, J. Stat. Mech. (2009) P09018.
[55] A. Honecker, F. Mila, and B. Normand, Multi-triplet bound states and finite-temperature dynamics in highly frustrated quantum spin ladders, Phys. Rev. B **94**, 094402 (2016).
[56] See Supplemental Material at http://link.aps.org/supplemental/10.1103/PhysRevB.96.060403 for momentum cuts of the spectral functions obtained from DMRG for different temperatures, spectral functions obtained from ED, QMC results for open boundary conditions, the finite-size scaling of the edge-state contribution, the thermal shift of the magnon peak, and the QMC results for the three-magnon continuum.
[57] C. Lanczos, An iteration method for the solution of the eigenvalue problem of linear differential and integral operators, J. Res. Natl. Bur. Stand. **45**, 255 (1950).
[58] E. Dagotto, Correlated electrons in high-temperature superconductors, Rev. Mod. Phys. **66**, 763 (1994).
[59] R. Haydock, V. Heine, and M. J. Kelly, Electronic structure based on the local atomic environment for tight-binding bands, J. Phys. C **5**, 2845 (1972).
[60] E. R. Gagliano and C. A. Balseiro, Dynamical Properties of Quantum Many-Body Systems at Zero Temperature, Phys. Rev. Lett. **59**, 2999 (1987).
[61] U. Schollwöck, The density-matrix renormalization group, Rev. Mod. Phys. **77**, 259 (2005).
[62] A. W. Sandvik, Computational studies of quantum spin systems, AIP Conf. Proc. **1297**, 135 (2010).
[63] A. C. Tiegel, S. R. Manmana, T. Pruschke, and A. Honecker, Matrix product state formulation of frequency-space dynamics at finite temperatures, Phys. Rev. B **90**, 060406(R) (2014); **94**, 179908(E) (2016).
[64] U. Schollwöck, The density-matrix renormalization group in the age of matrix product states, Ann. Phys. (N.Y.) **326**, 96 (2011).
[65] F. Verstraete, J. J. García-Ripoll, and J. I. Cirac, Matrix Product Density Operators: Simulation of Finite-Temperature and Dissipative Systems, Phys. Rev. Lett. **93**, 207204 (2004).
[66] A. E. Feiguin and S. R. White, Finite-temperature density matrix renormalization using an enlarged Hilbert space, Phys. Rev. B **72**, 220401(R) (2005).
[67] T. Barthel, U. Schollwöck, and S. R. White, Spectral functions in one-dimensional quantum systems at finite temperature using the density matrix renormalization group, Phys. Rev. B **79**, 245101 (2009).
[68] S. M. Barnett and B. J. Dalton, Liouville space description of thermofields and their generalisations, J. Phys. A: Math. Gen. **20**, 411 (1987).
[69] B. J. Dalton, Liouville space theory of sequential quantum processes. I. General theory, J. Phys. A: Math. Gen. **15**, 2157 (1982).
[70] A. Weiße, G. Wellein, A. Alvermann, and H. Fehske, The kernel polynomial method, Rev. Mod. Phys. **78**, 275 (2006).
[71] A. Holzner, A. Weichselbaum, I. P. McCulloch, U. Schollwöck, and J. von Delft, Chebyshev matrix product state approach for spectral functions, Phys. Rev. B **83**, 195115 (2011).
[72] A. Braun and P. Schmitteckert, Numerical evaluation of Green's functions based on the Chebyshev expansion, Phys. Rev. B **90**, 165112 (2014).
[73] H. Benthien, F. Gebhard, and E. Jeckelmann, Spectral Function of the One-Dimensional Hubbard Model Away from Half Filling, Phys. Rev. Lett. **92**, 256401 (2004).
[74] O. F. Syljuåsen and A. W. Sandvik, Quantum Monte Carlo with directed loops, Phys. Rev. E **66**, 046701 (2002).
[75] F. Alet, S. Wessel, and M. Troyer, Generalized directed loop method for quantum Monte Carlo simulations, Phys. Rev. E **71**, 036706 (2005).
[76] A. W. Sandvik, R. R. P. Singh, and D. K. Campbell, Quantum Monte Carlo in the interaction representation: Application to a spin-Peierls model, Phys. Rev. B **56**, 14510 (1997).
[77] F. Michel and H.-G. Evertz, Lattice dynamics of the Heisenberg chain coupled to finite frequency bond phonons, arXiv:0705.0799.
[78] K. S. D. Beach, Identifying the maximum entropy method as a special limit of stochastic analytic continuation, arXiv:cond-mat/0403055.
[79] S. Notbohm, D. A. Tennant, B. Lake, P. C. Canfield, J. Fielden, P. Kögerler, H.-J. Mikeska, C. Luckmann, and M. T. F. Telling, Temperature effects on multi-particle scattering in a gapped quantum magnet, J. Magn. Magn. Mater. **310**, 1236 (2007).
[80] A. J. A. James, F. H. L. Essler, and R. M. Konik, Finite-temperature dynamical structure factor of alternating Heisenberg chains, Phys. Rev. B **78**, 094411 (2008).
[81] D. A. Tennant, B. Lake, A. J. A. James, F. H. L. Essler, S. Notbohm, H.-J. Mikeska, J. Fielden, P. Kögerler, P. C. Canfield, and M. T. F. Telling, Anomalous dynamical line shapes in a quantum magnet at finite temperature, Phys. Rev. B **85**, 014402 (2012).